Journal of Cultural Heritage 29 (2018) 75–81

Available online at
ScienceDirect
www.sciencedirect.com

Elsevier Masson France
EM|consulte
www.em-consulte.com/en

Original article

Subsea spectral identification of shipwreck objects using laser-induced breakdown spectroscopy and linear discriminant analysis

Marina López-Claros, Francisco Javier Fortes, José Javier Laserna*

Universidad de Málaga, Facultad de Ciencias, Departamento de Química Analítica, Campus de Teatinos s/n, 29071 Málaga, Spain

ARTICLE INFO

Article history:
Received 7 September 2016
Accepted 20 December 2016
Available online 27 July 2017

Keywords:
Laser-induced breakdown spectroscopy
LIBS
Underwater analysis
Multi-pulse excitation
Optical fiber
Cultural heritage

ABSTRACT

Underwater LIBS is an evolving technology which offers unique advantages over traditional methods, not only do it offers the composition of liquids with high reliability; it also provides the elemental composition of solids with little or no user manipulation. Because of this advantage, LIBS has been used as a tool for inspecting materials in underwater archaeology, where knowledge of the chemical composition may provide valuable clues on the origin of materials in shipwrecks and submerged buildings. This study attempts to provide undersea LIBS instrumentation with the data processing tools intended to make shipwreck inspection surveys easier and faster. The new tool has been designed to sort the readings obtained by a LIBS system when inspecting unknown pieces found in the sea bottom and assign their composition to one of several groups of common materials found in shipwrecks. The tool involves linear discriminant analysis that was first validated in the laboratory with a training set of samples collected from wreckages. Then, the method was used in an underwater survey in the Mediterranean Sea to sort the materials found in a shipwreck. In combination with high-definition video recording, this approach can provide an understanding of the materials and a permanent record of the unknown assets, this eliminating the need for underwater archaeologists to make handwritten notes of individual pieces while surveying shipwrecks.

1. Introduction

Underwater cultural heritage is a rich source of information and a window to the past. In fact, the presence of specific elements (either greater or lesser percentage) in an archaeological material, namely chemical fingerprints, is of great interest for a better understanding of its age, provenance and manufacturing technology. Discovery of amphoras, cannons and metallic artefacts in their archaeological context could provide further information concerning the age and nationality of a shipwreck [1]. However, the severe conditions of the marine environment change the appearance of the underwater sites and distorts the idyllic image of the shipwreck until blending with the surroundings. Hence, artefacts and structures may be uncovered beneath sediments, chemically altered or even destroyed.

Recent advances in electronic engineering, underwater robotics and novel systems for processing and image recognition make localization of underwater archaeological sites much easier than in past. However, underwater archaeology still requires the development of screening techniques for the in-situ recognition of findings. A restricted number of laser-based techniques (i.e. Raman, LIBS and LIF) have proven to be useful for this purpose [2–4]. Specifically, LIBS is really appreciated as is the unique that could provide atomic information from the spectral signature of underwater objects [5,6]. Additionally, LIBS combines valuable attributes (no sample preparation, minimally destructive, fast analytical response and possibility of remote sensing analysis), specially demanded in cultural heritage preservation and investigation [7,8]. It's worth mentioning that underwater LIBS analysis is not a trivial task and several research groups have proposed different alternatives for improving LIBS sensitivity inside liquids [9–11]. In this sense, the dual pulse excitations being the most common approach proposed in the literature [12–14]. However, problems related to the use of two laser sources, the precise alignment needed and synchronization in data acquisition are obstacles for its implementation in field analysis [15,16]. The instrumental development was further investigated until 2012 when Guirado et al. [17] published the first in-situ undersea LIBS analysis of solid materials, at a depth of 30 m,

---

* Corresponding author. Tel.: +34 951953007.
E-mail address: laserna@uma.es (J.J. Laserna).

https://doi.org/10.1016/j.culher.2016.12.015
1296-2074/

using a fiber-based LIBS system. Later, a new generation of LIBS instruments based on transmission of a collinear sequence of multi-pulses through the optical fiber cable was proposed by the same authors to improve the performance of the technology [18,19]. An archaeological shipwreck situated 17 m deep was inspected using this approach [20].

In subaquatic archaeology, quantitative information turns crucial for planning restoration/conservation activities and taking decisions about whether the object should be moved from the underwater site or not. Nevertheless, LIBS strongly depends on matrix effects, pulse to pulse fluctuations, plasma-solid interactions, among other factors. In this sense, a broad number of fundamental studies have been reported to overcome the so-called fractionation effect [21–24]. Certain procedures such as internal standardization, background normalization, calibration-free analysis and the use of a double-pulse configuration has been explored so far for quantitative analysis of submersed materials. Most recently, Guirado et al. [25] evaluated the use of multi-pulse (MP) excitation as an effective solution to mitigate the fractionation effects observed in LIBS analysis of copper-based alloys. MP-LIBS also prevents the effect of ambient pressure on LIBS signal, thus demonstrating the feasibility of LIBS for quantitative analysis of bronze materials in a real underwater site.

In such a scenario, development of spectral libraries and data processing algorithms also improve the capability of LIBS for field measurements. Hence, from an archaeological point of view, both qualitative and quantitative information extracts compositional evidence that together with the use of chemometric methods may identify specific materials which could be related to ancient manufacturing or production processes [26]. A number of statistical methods including linear and rank correlation, principal component analysis (PCA), partial least-squares discriminant analysis (PLS-DA) and soft independent modeling of class analogy (SIMCA), among others have proved to group and classify ancient artefacts in archaeometric analysis [27]. In this work, a classification method is evaluated for the identification of chemical fingerprints in shipwrecks. A variety of archaeological objects has been previously characterized in laboratory using essentially the same operational conditions than those found undersea in order to ensure the effectiveness of the method during the recognition process in the site. Moreover, a set of sheathings from different shipwrecks were analyzed with the objective to perform a chronocultural sorting of these structural pieces. Based on this procedure, findings from the shipwreck of *San Pedro de Alcántara* (Malaga, Spain) were directly classified into metallic alloys, ceramics, rocks or marbles.

2. Materials and methods

The remote LIBS instrument and its construction have been described in a recent paper [20] so only a brief description of the instrument is given here. The system consists of two well-defined parts: a hand-held probe and a main unit, interconnected by means of an umbilical cable. The main unit comprises the optical module for laser-fiber coupling, the data acquisition module and the laser power supply.

The optical module consists of a polymethyl methacrylate structure, specially adapted in order to prevent the deposition of particles from the marine environment at the tip of the optical fiber. The module contains the laser head (Q-switched Nd:YAG laser operating at 1064 nm, Brilliant) and all the optical arrangements for launching the laser radiation into the fiber-optic cable (mounted in a *xyz* stage) and collecting the plasma light for the transmission to a spectrograph. The laser beam is transmitted through a 55-m long fiber optic cable that travels inside an umbilical cord which connects the probe to the optical module. At the end of the fiber, the hand-held probe focuses the laser beam onto the sample surface by an appropriate optical configuration. With this configuration, the spot size was established at 450 μm in diameter.

The same optical fiber is used for light gathering purposes. The plasma light is collected and returned to the optical module, where it is conducted to the data-acquisition module using an optical system used to focus plasma light into the spectrometer fiber-optic cable (2 m length, 600 μm diameter, NA0.22). The data-acquisition module, consisting of the spectrometer, the video converter and the PC components, was installed in the main unit. A pulse/delay generator (which externally controls the system) was also configured within this module. The spectrometer is a crossed Czerny-Turner design with a holographic diffraction grating of 1200 lines mm^{-1} (Avantes, model AvaSpec-2048-USB2). This configuration provides a spectral resolution of 0.1–0.2 nm/pixel in the spectral range of 300–550 nm. AvaSoft software was employed for controlling the spectrometer and for data processing. The acquisition delay was established in 1 μs which corresponds to the best signal-to-noise ratio (SNR) for the LIBS signal. The irradiance value at sample surface was 1.6 GW cm^{-2}. And all underwater analysis was carried out using 5 bars of argon as a purge gas. The Statgraphics® statistics software package was used for chemometrics analysis.

3. Results and discussion

3.1. Classification method for archaeological artefacts

Given the great compositional diversity, textural differences and surface alteration of the submersed cultural heritage, the use of advanced statistical algorithms is essential for the recognition and sorting of underwater findings. For this purpose, linear discriminant analysis (LDA) was used to generate a classification model from which unknown samples will be predicted in site on the basis of their LIBS response. As a supervised algorithm, a LDA model based on the spectra acquired from a set of known archaeological samples was constructed. LDA evaluates the relative weights of the original variables for group discrimination and score the separation between multiple classes [28–30]. Afterwards, the model predicts the probability that an unknown sample belongs to each class.

A set of 38 objects collected from several archaeological shipwrecks was first studied. To simulate the experimental conditions of a subsea environment, samples were immersed and analyzed in a water tank in our laboratory. Because of the large variety of samples used in this study, objects were divided into different groups for chemometric analysis, i.e. bronze-alloys (10 samples), metallic pieces (18 samples), ceramics (5 samples) and marbles (5 samples). LIBS spectra were acquired in the 350–550 nm spectral range and their intensities normalized to unity for comparative purposes. Data were acquired by averaging the response of 50 laser shots on three adjacent positions for each sample. However, the whole LIBS spectra were not considered as input data. From the initial information of 2048 data points, only 10 spectral variables were considered for analysis. The selected variables were Cu (I) 510.55 nm, Zn (I) 481.05 nm, Sn (I) 452.47 nm, Pb (I) 405.78 nm, Fe (I) 438.35 nm, Ca (I) 422.67 nm, Mg (I) 517.26 nm, Si (I) 390.55 nm, Sr (I) 407.61 nm and Ti (I) 498.17 nm. In addition, the presence of Ca, Mg, Si and Ti in metallic samples is associated to the deposition of sedimentary material on the sample surface. The first discriminant function has the expression:

$$F1 = 2.7 \cdot I_{Cu} + 2.4 \cdot I_{Zn} + 22.8 \cdot I_{Sn} + 0.8 \cdot I_{Pb} + 2.7 \cdot I_{Fe} - 7.2 \cdot I_{Ca} - 1.2 \cdot I_{Mg} - 3.8 \cdot I_{Sr} - 6.0 \cdot I_{Si+Ti} + 0.59$$

Table 1
Prediction groups membership for training set samples. ID sample is constitutes by a letter and two numbers as follows: the letter represents the type of sample (A: copper based alloy; M: metal; C: ceramic; B: marble), the first number corresponds to the shipwreck (I: Delta II, II Delta III) and the second to a number in the group classified.

ID	Prediction group membership (%)					ID	Prediction group membership (%)				
	Alloy	Metal	Ceramic	Marble	Total		Alloy	Metal	Ceramic	Marble	Total
AII1	100	0	0	0	100	MI12	0	100	0	0	100
AII2	100	0	0	0	100	MI13	0	100	0	0	100
AI1	100	0	0	0	100	MI14	0	100	0	0	100
AI2	100	0	0	0	100	MI15	0	100	0	0	100
AI3	100	0	0	0	100	MI16	0	100	0	0	100
AII3	100	0	0	0	100	MI17	0	100	0	0	100
AII4	99.4	0.6	0	0	100	MII9	0	100	0	0	100
AII5	100	0	0	0	100	MI18	0	100	0	0	100
AI4	99.9	0.1	0	0	100	MII10	4.2	95.8	0	0	100
AII6	94.7	5.3	0	0	100	CI19	0	0	100	0	100
MII7	3.3	96.7	0	0	100	CI20	0	0	100	0	100
MII8	0	100	0	0	100	CI21	0	0	100	0	100
MI5	0	100	0	0	100	CI22	0	0	100	0	100
MI6	0	100	0	0	100	CI23	0	0	100	0	100
MI7	0	100	0	0	100	B1	0	0	0	100	100
MI8	0	100	0	0	100	B2	0	0	0	100	100
MI9	0	100	0	0	100	B3	0	0	0	100	100
MI10	0	100	0	0	100	B4	0	0	0.2	99.8	100
MI11	0	100	0	0	100	B5	0	0	0	100	100

where I_n is the intensity of each element line. This function has an excellent canonical correlation, 0.98, that is its relative ability to discriminate amongst the groups. The second function is:

$$F2 = 1.8 \cdot I_{Cu} + 3.8 \cdot I_{Zn} + 24.8 \cdot I_{Sn} - 0.2 \cdot I_{Pb} - 0.8 \cdot I_{Fe} + 2.5 \cdot I_{Ca} - 1.8 \cdot I_{Mg} - 1.5 \cdot I_{Sr} + 9.4 \cdot I_{Si+Ti} - 2.0$$

which also exhibits a good canonical correlation (0.91). Nevertheless, the statistics treatment scores Wilk's lambda values of 0.0013 for F_1 and 0.03 for F_2, which suggests that the variables selected for the linear discriminant analysis are appropriate for sample discrimination. Both functions also have a very high significance level of Chi^2 statistics, 201 and 106 for F_1 and F_2, respectively.

The coefficients associated to different elements calculated by the software for discriminant functions give information about the relative contribution of each spectral line to the separation of groups. Thus, large coefficient values, such as those associated to Sn or Si ± Ti spectral lines, contribute to a larger extent to group discrimination. For instance, tin is present in alloys whereas it is virtually absent in metals, ceramics and marbles. The software then assigns a large coefficient to this element to enable the separation of alloys from the other groups. Similarly, Si and Ti help in the separation of ceramics. Since the lines of these elements in the selected spectral window are weak, the intensities were summed to allow a better separation.

Positive and negative coefficients also contribute to separation among groups. The LDA software assigns positive coefficients to the alloying elements in bronzes and metallic pieces; in contrast, negative coefficients characterize strongly dissimilar materials such as ceramics and marbles.

The classification functions generated by the proposed model were validated with the training set of samples. Table 1 summarizes the classification of each sample based on the proposed model. It's worth mentioning that all samples were identified without exceptions. A scatter plot of the first two discriminant functions is presented in Fig. 1. As shown, samples are separated in four classes or groups attending to the type of material previously described in the "supervised" model. Bronze alloys and metallic pieces are grouped in the right-hand side of the graph, whereas ceramics and marbles are grouped in the second and third quadrant of the scatter graph, respectively. The centroid of each group is also marked in the graph. The model has been checked in our laboratory with a set of sheathings simulating the experimental conditions of a subsea environment. Furthermore, it has been tested during the underwater inspection of the wreck of San Pedro de Alcantara.

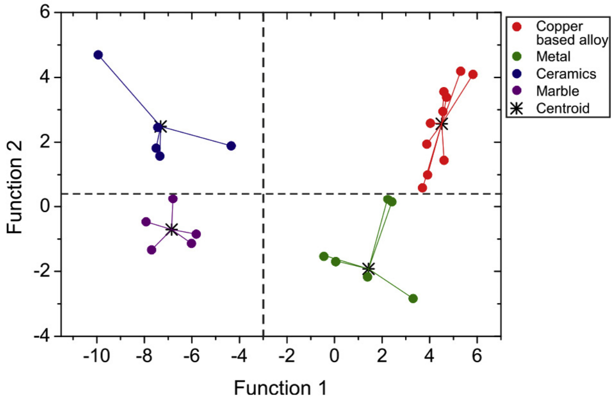

Fig. 1. Scatter plot of the first two canonical discriminant functions containing the four groups defined in the method.

3.2. Chronological sorting of metallic sheathings

Since the Phoenician times, the use of sheathings in wooded-hulled vessels has been extensively tested to prevent wood degradation by the action of seawater, bivalve molluscs and algae. Sheathings were also used to improve the operability of the boat. The type of sheathing has evolved with time so the knowledge of elemental composition of this kind of samples makes it possible the assignment of the manufacturing period and provides clues to uncover the ship's origin [31].

A set of sheathing pieces belonging to different shipwrecks were analyzed in a water tank in an attempt to provide information about the geographical origin of the shipwreck that could be helps us to understand its historical context. In addition, this set of four samples will be used to evaluate in laboratory our chemometric model described in Section 3.1. Samples were found in the underwater archaeological sites of "*Delta I*" (XVII century, Spanish), "*Delta II*" (XVI century, Italian), "*Mercante de San Sebastian*" (XVIII century, Spanish) and "*Fougueaux*" (XVIII century, French). A chronocultural

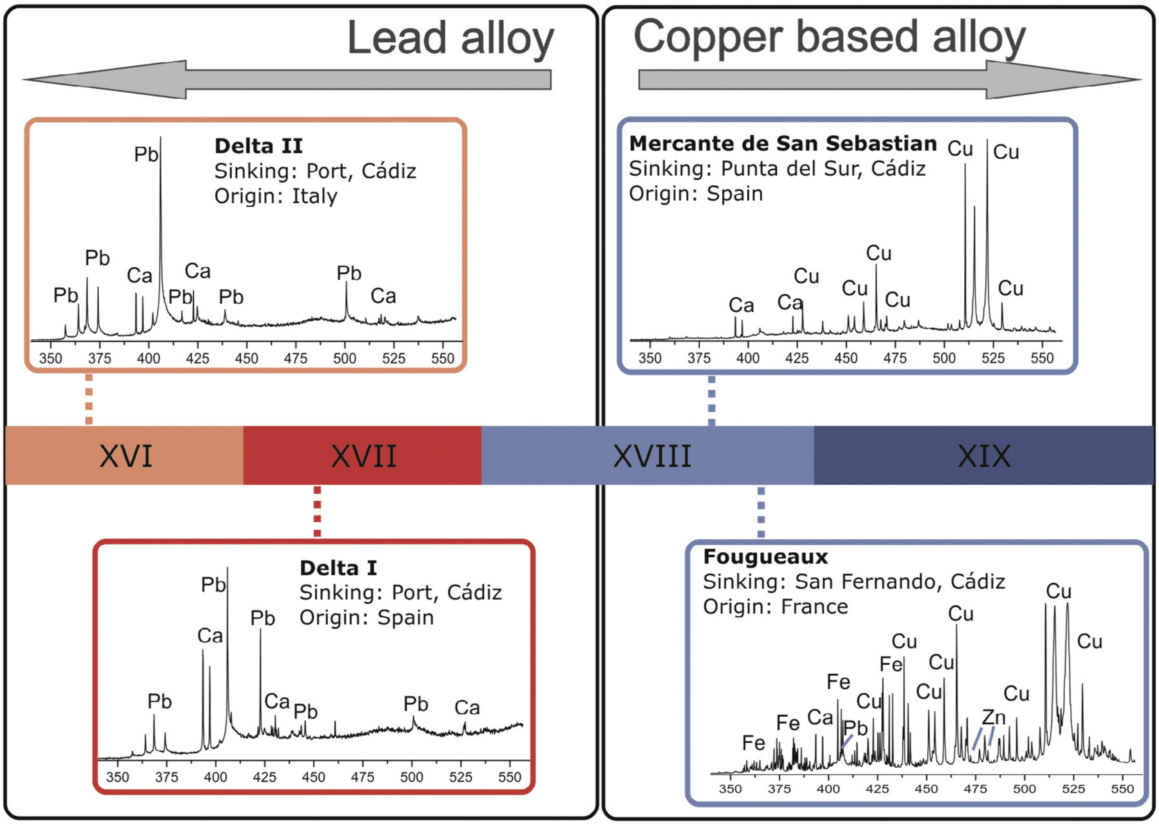

Fig. 2. Chronocultural sorting of evolution of sheathing's composition from lead to copper based alloys. The main emission lines are labeled in the spectra.

sorting of the sheathings analyzed by LIBS is presented in Fig. 2. The main emission lines are labeled in the spectra. As seen, the squares limit the timeline in two periods, depending on the sheathing composition. Thus, lead-based sheathings were early introduced in the XV century in Portuguese and Spanish arsenals and its use was extended until the XVII century [31]. This fact is easily observed in the sheathings belonging to *Delta I* and *Delta II*, as revealed by the LIBS spectra sketched in the figure. In the XVIII century, lead-based sheathings were substituted first by copper and then by copper-based alloys. As shown in Fig. 2, the LIBS spectra of *Mercante de San Sebastian* and *Fougueaux* in chronological order. In addition, the presence of minor components such as zinc, iron or lead, as observed in the spectrum corresponding to the *Fougueaux*, could indicate its country of origin. Hence, it exists a clear evolution of the sheathing's composition from lead to copper based alloys that could be related to a period of history or even to the country of manufacture of the shipwreck.

On the other hand, the intensity of emission lines of this set of sheathings has been used to check in laboratory our LDA model proposed in Section 3.1 using samples different to the training set. In this case, the discriminant functions (F1 and F2) have been able to assign successfully the samples as metallic sheatings corresponding to *Delta I*, *Delta II* and *Mercante de San Sebastian* and a bronze-alloy as part of the *Fougueaux*.

3.3. *Identification of objects in shipwrecks. The wreck of* San Pedro de Alcantara

The wreck of *San Pedro de Alcantara*, located in the South of Spain, was discovered 10 m deep over a sandy bottom area. The wreck presents a military-structure type with a beam of 60 m, 10–12 m of breadth. The structure of the boat is covered by sediments, calcareous deposits and marine algae. Prior to the LIBS measurement campaign, a site survey was accomplished by the archaeologists from the Centro de Arqueología Subacuática de cádiz (CAS) who located archaeological pieces from the remains of the wreck and removed the concretion layer from the sample surface.

The LIBS instrument was deployed on the vessel's board while a diver operated the LIBS probe in the sea bottom. The input pressure for underwater analysis was set to 5 bars, the maximum pressure supported by the system. The use of a gas purge is of key importance for preventing the admittance of water into the LIBS probe and create a solid-gas interface for LIBS analysis. Given the high alteration degree of the samples inspected, we decided to use argon as a purge gas, which provided a larger LIBS intensity when compared to air.

A large number of archaeological objects were discovered and analyzed by LIBS during the survey. Fig. 3 shows parts of the shipwreck and the LIBS probe operated by a diver. To assign the typical spectrum of a material and in order to ensure the reproducibility of the results, data were acquired by averaging the response of 50 laser shots on three adjacent positions for each sample. Then, acquired spectral intensities were normalized to unity for comparative purposes. Each object exhibits a distinctive chemical that was introduced in the classification method developed in Section 3.1. From the canonical discriminant functions described there, the unknown findings from the wreck were grouped into several categories easily. Fig. 4 presents the classification of the set of unknown objects. As shown, samples from the subsea archaeological site were unequivocally classified in each of the aforementioned groups. The scatter points (in grey color) from the set of samples employed for modeling the classification method are also plotted in the graph. Results for the unknown samples classification are summarized in Table 2. Objects were correctly identified as four bronze alloys, eight ceramic fragments, seven metallic pieces and four marbles.

Table 2
Prediction groups membership for unknown samples. ID sample is constitutes by a letter represents the type of sample (A: copper based alloy; M: metal; C: ceramic; B: marble) and a number in the group classified.

ID	Prediction group membership (%)					ID	Prediction group membership (%)				
	Alloy	Metal	Ceramic	Marble	Total		Alloy	Metal	Ceramic	Marble	Total
A1	100	0	0	0	100	C4	0	0	100	0	100
A2	100	0	0	0	100	C5	0	0	100	0	100
A3	100	0	0	0	100	C6	0	0	100	0	100
A4	99.4	0.6	0	0	100	C7	0	0	100	0	100
M1	0	100	0	0	100	C8	0	0	100	0	100
M2	0	91.2	0	8.8	100	M8	0	100	0	0	100
M3	0	100	0	0	100	M9	0	100	0	0	100
M4	0	100	0	0	100	M10	13	87	0	0	100
M5	0	100	0	0	100	A5	88.7	11.3	0	0	100
M6	0	100	0	0	100	B1	0	0	0.5	99.5	100
M7	0	100	0	0	100	B2	0	0	0	100	100
C1	0	0	100	0	100	B3	0	0	0	100	100
C2	0	0	100	0	100	B4	0	0	0	100	100
C3	0	0	100	0	100						

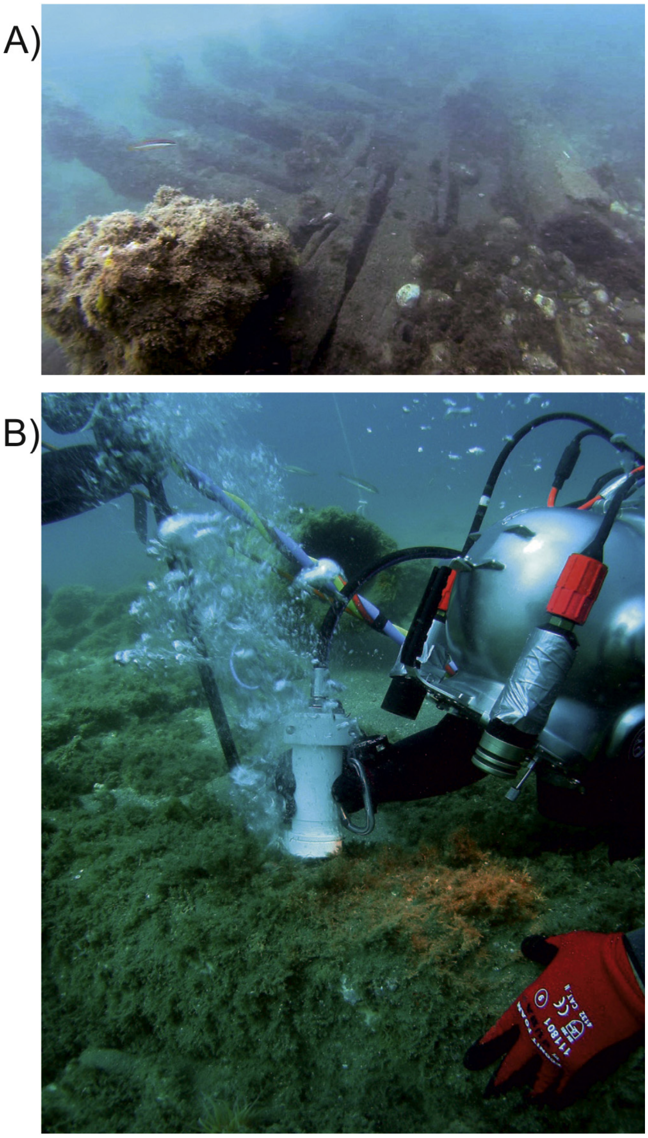

Fig. 3. Photographic detail of the structure of the boat (A), and diver operating the LIBS probe in the wreck of *San Pedro Alcántara* (B).

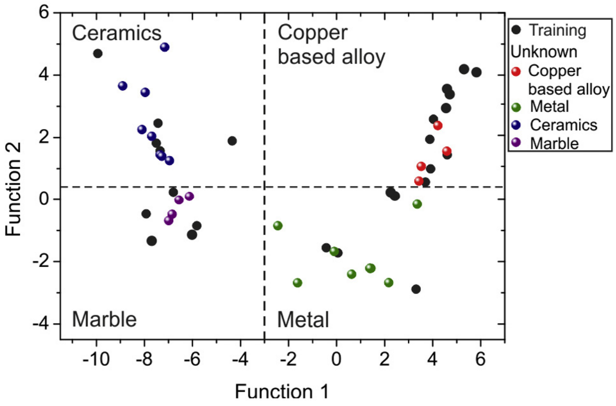

Fig. 4. Classification scatter plot of the first two canonical discriminant functions of modeling developed. The scatter points in grey color corresponds to the set of samples employed for modeling the classification method and colored spheres represents the set of unknown objects.

Fig. 5 shows a drawing top view of the shipwreck in which the bow is oriented to the northwest position and the aft, to the southeast. The drawing describes the state of conservation of the wreck, where the shipwreck structure is observed, as well as the way is distributed along the site. The locations of the archaeological pieces are also indicated. Chemical composition of each object is detailed as a bar diagram inset. As shown, various types of samples were identified as defense material such as two iron canons (M2, M4) and a canon bullet (M3) composed of iron with manganese as a minor constituent. On the other hand, pieces of crew clothing present a chemical composition based on copper alloy with zinc in the case of jacquet button (A2) and zinc-lead in the case of the belt buckle (A4). Regarding to ceramic fragments, in general, are constituted by calcium, magnesium, aluminum, iron, silicon, strontium and titanium; although pieces C3, C5 and C7 also contained lead. Some unidentified pieces show a variable chemical composition such as metals copper-lead (A3) alloy, and copper-zinc-lead (A1) alloy; and lead (M1, M7) or iron (M5, M6) metals.

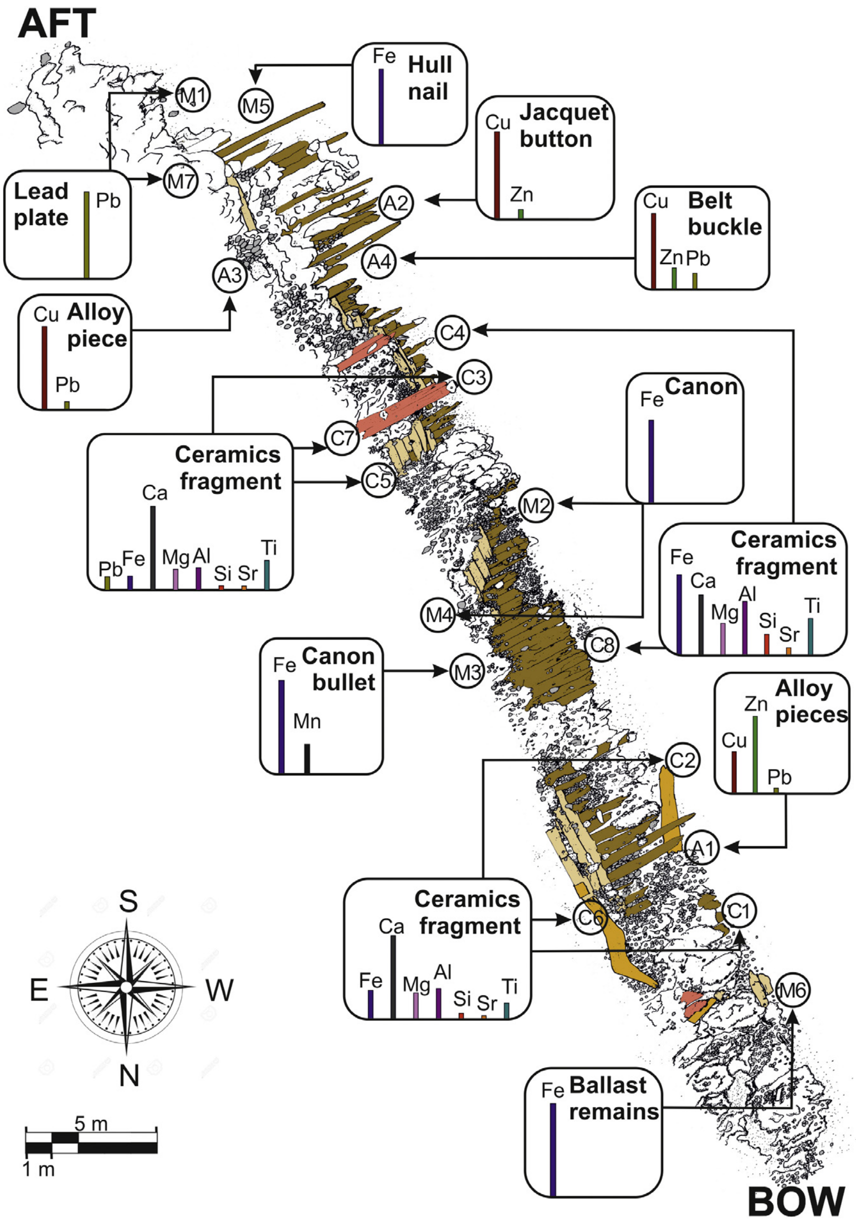

Fig. 5. Schematic drawing of the shipwreck. The inset bar diagrams represent the chemical composition of each object and the locations of the archaeological findings.

4. Conclusions

Using a LIBS sensor deployed on a small vessel, a hand-held probe was submersed by a diver to the shipwreck of San Pedro de Alcantara located in the South of Spain over the Mediterranean Sea. LIBS data from a variety of objects found in the wreck were collected, logged and accurately geo-positioned for post survey analysis. In addition to metallic objects, refractory materials such as rocks and ceramics were analyzed. Although algae and calcareous deposits had to be removed from the sample surface before the analysis, the LIBS system constitutes a significant step forward, allowing the acquisition of a consistent set of spectral data that can be treated by a software based on linear discriminant analysis for assigning the chemical identity of the object. The information thus gathered provides valuable data on the identity of shipwrecks located in coastal waters.

Acknowledgments

This research was funded by Junta de Andalucía, Consejería de Economía, Innovación, Ciencia y Empleo through project P11-FQM-7193 (AQUALAS), a joint effort of Instituto Andaluz del Patrimonio Histórico (IAPH), Centro de Arqueología Subacuática (CAS) and the University of Malaga (UMA). M. Lopez-Claros would like to acknowledge the Consejería de Innovación, Ciencia y Empleo of the Junta de Andalucía for her fellowship. Authors would also like to acknowledge the valuable assistance of Salvador Guirado and at the same time the huge ability to commit, work and peerless dedication of CAS's archaeologists Carmen García Rivera, Milagros Alzaga, Josefa Martí, Nuria Rodríguez and Aurora Higueras-Milena.

References

[1] C. Pearson, Conservation of marine archaeological objects, Butterworth & Co. Ltd, London, 1987.

[2] X. Zhang, W.J. Kirkwood, P.M. Walz, E.T. Peltzer, P.G. Brewer, A review of advances in deep-ocean Raman spectroscopy, Appl. Spectrosc. 66 (2012) 237–249.

[3] B. Thornton, T. Takahashi, T. Sato, T. Sakka, A. Tamura, A. Matsumoto, T. Nozaki, T. Ohki, K. Ohki, Development of a deep-sea laser-induced breakdown spectrometer for in situ multi-element chemical analysis, Deep. Res. Part I 95 (2015) 20–36.

[4] R. Fantoni, R. Barbini, F. Colao, D. Ferrante, L. Fiorani, A. Palucci, Integration of two lidar fluorosensor payloads in submarine ROV and flying UAV platforms, EARSeL eProc. 3 (2004) 43–53.

[5] F.J. Fortes, J. Moros, P. Lucena, L.M. Cabalín, J.J. Laserna, Laser-induced breakdown spectroscopy, Anal. Chem. 85 (2013) 640–669.

[6] R.E. Russo, X. Mao, J.J. Gonzalez, V. Zorba, J. Yoo, Laser ablation in analytical chemistry, Anal. Chem. 85 (2013) 6162–6177.

[7] A. Giakoumaki, K. Melessanaki, D. Anglos, Laser-induced breakdown spectroscopy (LIBS) in archaeological science – applications and prospects, Anal. Bioanal. Chem. 387 (2007) 749–760.

[8] V. Spizzichino, R. Fantoni, LIBS in archaeometry: a review of its application and future perspectives, Spectrochim. Acta Part B 99 (2014) 201–209.

[9] V. Lazic, F. Colao, R. Fantoni, V. Spizzicchino, Recognition of archeological materials underwater by laser induced breakdown spectroscopy, Spectrochim. Acta Part B 60 (2005) 1014–1024.

[10] V. Lazic, S. Jovićević, Laser induced breakdown spectroscopy inside liquids: Processes and analytical aspects, Spectrochim. Acta Part B 101 (2014) 288–311.

[11] T. Sakka, H. Oguchi, S. Masai, K. Hirata, Y.H. Ogata, Use of a long-duration ns pulse for efficient emission of spectral lines from the laser ablation plume in water, Appl. Phys. Lett. 88 (2006) 061120.

[12] V. Lazic, J.J. Laserna, S. Jovicevic, Insights in the laser induced breakdown spectroscopy signal generation underwater using dual pulse excitation — Part II: plasma emission intensity as a function of interpulse delay, Spectrochim. Acta Part B 82 (2013) 50–59.

[13] V. Lazic, J.J. Laserna, S. Jovicevic, Insights in the laser-induced breakdown spectroscopy signal generation underwater using dual pulse excitation — Part I: vapor bubble, shockwaves and plasma, Spectrochim, Acta Part B 82 (2013) 42–49.

[14] A. De Giacomo, M. Dell'Aglio, O. De Pascale, M. Capitelli, From single pulse to double pulse ns-laser induced breakdown spectroscopy under water: elemental analysis of aqueous solutions and submerged solid samples, Spectrochim. Acta Part B 62 (2007) 721–738.

[15] F.J. Fortes, J.J. Laserna, The development of fieldable laser-induced breakdown spectrometer: no limits on the horizon, Spectrochim. Acta Part B 65 (2010) 975–990.

[16] F.J. Fortes, S. Guirado, A. Metzinger, J.J. Laserna, A study of underwater stand-off laser-induced breakdown spectroscopy for chemical analysis of objects in the deep ocean, J. Anal. At. Spectrom. 30 (2015) 1050–1056.

[17] S. Guirado, F.J. Fortes, V. Lazic, J.J. Laserna, Chemical analysis of archeological materials in submarine environments using laser-induced breakdown spectroscopy. On-site trials in the Mediterranean Sea, Spectrochim. Acta Part B 74–75 (2012) 137–143.

[18] L.M. Cabalín, A. González, V. Lazic, J.J. Laserna, Deep ablation and depth profiling by laser-induced breakdown spectroscopy (LIBS) employing multi-pulse laser excitation: application to galvanized steel, Appl. Spectrosc. 65 (2011) 797–805.

[19] S. Guirado, F.J. Fortes, L.M. Cabalín, J.J. Laserna, Effect of pulse duration in multi-pulse excitation of silicon in laser-induced breakdown spectroscopy (LIBS), Appl. Spectrosc. 68 (2014) 1060–1066.

[20] S. Guirado, F.J. Fortes, J.J. Laserna, Elemental analysis of materials in an underwater archeological shipwreck using a novel remote laser-induced breakdown spectroscopy system, Talanta 137 (2015) 182–188.

[21] R. Fantoni, L. Caneve, F. Colao, L. Fornarini, V. Lazic, V. Spizzichino, Methodologies for laboratory laser induced breakdown spectroscopy semi-quantitative and quantitative analysis – a review, Spectrochim. Acta Part B 63 (2008) 1097–1108.

[22] A. De Giacomo, M. Dell'Aglio, A. Casavola, G. Colonna, O. De Pascale, M. Capitelli, Elemental chemical analysis of submerged targets by double-pulse laser-induced breakdown spectroscopy, Anal. Bioanal. Chem. 385 (2006) 303–311.

[23] S. Almaviva, R. Fantoni, L. Caneve, F. Colao, L. Fornarini, A. Santagata, R. Teghil, Use of ns and fs pulse excitation in laser-induced breakdown spectroscopy to improve its analytical performances: a case study on quaternary bronze alloys, Spectrochim. Acta B 99 (2014) 185–192.

[24] E. Tognoni, G. Cristoforetti, S. Legnaioli, V. Palleschi, Calibration-free laser-induced breakdown spectroscopy: state of the art, Spectrochim. Acta Part B 65 (2010) 1–14.

[25] S. Guirado, F.J. Fortes, J.J. Laserna, Multi-pulse excitation for underwater analysis of copper-based alloys using a novel remote laser-induced breakdown spectroscopy system, Appl. Spectrosc. 70 (2016) 618–626.

[26] M.J. Baxter, Exploratory multivariate analysis in archaeology", Edinburgh University Press, Edinburgh, 1994.

[27] M. Corsi, G. Cristoforetti, M. Giuffrida, M. Hidalgo, S. Legnaioli, L. Masotti, V. Palleschi, A. Salvetti, E. Tognoni, C. Vallebona, A. Zanini, Archaeometric analysis of ancient copper artefacts by laser-induced breakdown spectroscopy technique, Microchim. Acta 152 (2005) 105–111.

[28] J.B. Sirven, B. Sallé, P. Mauchien, J.L. Lacour, S. Maurice, G. Manhès, Feasibility study of rock identification at the surface of Mars by remote laser-induced breakdown spectroscopy and three chemometric methods, J. Anal. At. Spectrom. 22 (2007) 1471.

[29] J.L. Gottfried, R.S. Harmon, F.C. De Lucia, A.W. Miziolek, Multivariate analysis of laser-induced breakdown spectroscopy chemical signatures for geomaterial classification, Spectrochim. Acta Part B 64 (2009) 1009–1019.

[30] F. Colao, R. Fantoni, P. Ortiz, M.A. Vazquez, J.M. Martin, R. Ortiz, N. Idris, Quarry identification of historical building materials by means of LIBS XRF and chemometric analysis, Spectrochim. Acta Part B 65 (2010) 688–694.

[31] M. Bethencourt, A. Bocalandro, J. Romero-Pastor, Datación de pecios de los siglos XVIII y XIX a través de la caracterización de los forros de cobre, in: IV Congreso Latinoamericano de Conservación y Restauración del Metal, Madrid, 13-17 September 2011, Secretaría General Técnica, Ministerio de Educación, Cultura y Deporte; Grupo Español de Conservación, Madrid, 2011, pp. 51–62.